

Charged scalars at finite electric field and temperature in the optimized perturbation theory

William R. Tavares,^{1,*} Rudnei O. Ramos,^{1,†} Ricardo L. S. Farias,^{2,‡} and Sidney S. Avancini^{3,§}

¹*Departamento de Física Teórica, Universidade do Estado do Rio de Janeiro, 20550-013 Rio de Janeiro, RJ, Brazil*

²*Departamento de Física, Universidade Federal de Santa Maria, 97105-900 Santa Maria, RS, Brazil*

³*Departamento de Física, Universidade Federal de Santa Catarina, 88040-900 Florianópolis, SC, Brazil*

We study the symmetry breaking and restoration behavior of a self-interacting charged scalar field theory under the influence of a constant electric field and finite temperature. Our study is performed in the context of the optimized perturbation theory. The dependence of the effective potential with constant electric fields is established by means of the bosonic propagators in the Schwinger proper-time method. Explicit analytical expressions for the electric and thermal contributions are found. Our results show a decreasing behavior for the vacuum expectation value as a function of the electric fields, which is strengthened by the temperature effect. A first-order phase transition that occurs at zero /weak electric fields changes to a second-order phase transition under strong electric fields. The critical temperature for the phase transition exhibited a very weak dependence on the electric field. Additionally, we computed the vacuum persistence probability rate for the interacting theory, finding a peak at the critical point. The maximum value of this rate at the critical point is found to be independent of the coupling constant but depended solely on the magnitude of the electric field.

I. INTRODUCTION

The study of physical systems through their symmetry aspects is a fundamental approach in modern physics. By defining an order parameter, we can investigate the different phases exhibited by a system [1, 2]. Understanding how these systems behave under the influence of external parameters, such as temperature, density, magnetic fields, or electric fields, is crucial for describing realistic scenarios with applications in fields like cosmology, condensed matter, and particle physics.

While the effects of magnetic fields on phase transitions have been extensively studied (see, for instance, Refs. [3–6] for reviews and references therein), research on the influence of electric fields is less common. Electric fields have significant applications in condensed matter systems, such as in the case of assisted Schwinger pair production [7]. This phenomenon occurs when an electric field aids in the creation of particle-antiparticle pairs near the Fermi surface. An example of this is graphene layers, which due to their unique electronic properties, offer opportunities to study similar vacuum structures as those found in quantum electrodynamics [8].

Much of the existing literature has focused on the effects of electric fields on the quantum chromodynamics (QCD) phase transition. Strong electromagnetic fields can be produced in peripheral heavy ion collisions [9–12] and in asymmetric collisions [13–15]. External magnetic fields play a significant role in heavy ion collisions at typical energies (e.g., at those energies achieved in the RHIC and ALICE colliders), where intensities of the

order $eB \sim 10^{19}$ G can be achieved [16]. Similar to magnetic fields, electric fields can serve as an interesting control parameter to study important aspects of QCD. Recent numerical analyses have been employing intermediate energy per nucleon pair, e.g., $\sqrt{s_{NN}} = 3 - 20$ GeV, in heavy ion collisions. These studies demonstrate that, due to baryon stopping, these energies can indeed play a crucial role in creating electric fields that persist long enough to modify important hadronic processes [17, 18]. Electromagnetic fields present in heavy ion collisions are also expected to influence the dynamics of quark-gluon plasma, such as through anomalous transport phenomena like the chiral magnetic effect [19] and chiral separation effect [16, 20].

In the context of application to QCD, it is expected that electric fields can suppress the chiral condensate [21, 22], even in the case of chromo-electric fields [23]. Also, chiral perturbation theory has some results concerning to the properties of nucleons and its decays in the weak field regime [24], but just only recently is that electric fields have been combined with temperatures in effective models, as the Nambu–Jona-Lasinio and its extensions [25–29], the linear sigma model coupled with quarks [30] and Dyson-Schwinger equations [31]. Those studies have indicated that the combined effects of temperature and electric fields tend to strengthen the restoration of the partial chiral symmetry, accompanied by the decrease of the pseudocritical temperature until $eE \sim 0.3$ GeV², where it starts to increase. Studies of the deconfinement transition have shown similar qualitative behavior to the chiral transition’s pseudocritical temperature [30]. Lattice approaches, on the other hand, have been applied in the case of imaginary electric fields [32]. However, recent new techniques have been used in order to avoid technical issues similar to the sign problem, such as the use of isospin electric charge in the Minkowskian electric field [33]. New research indicates that the deconfinement temperature increases with electric field strength [34], suggesting the

* tavares.william@ce.uerj.br

† rudnei.ramos@uerj.br

‡ ricardo.farias@ufsm.br

§ sidney.avancini@ufsc.br

need for refinements in model approaches.

While there have been attempts to study strongly interacting quark matter using chiral and deconfinement phase transitions in strong electric fields, there's a lack of research on charged scalar theories. Recent predictions for $\lambda\phi^4$ theories have been made using one-loop bosonic propagators in finite spatial confining systems [35] and through ring diagrams at low and high temperatures [36–38]. In the present paper, we use the method of the optimized perturbation theory (OPT) [39, 40] (see also, e.g., Ref. [41] for a recent review) to study the phase transition for a self-interacting complex scalar field model at finite temperature and in a constant electric field. The OPT is a nonperturbative method able to resum loop contributions in a self-consistent way. It has been so far applied to a large variety of problems, ranging from condensed matter systems [42–45], chiral phase transition in QCD effective models [46–49] and in quantum field theory in general [50–58]. It has been demonstrated that it has a fast convergence [59, 60], which is of particular importance, since already at first order the OPT is able to produce results improving over other nonperturbative methods, e.g., the large- N expansion and Gaussian approximations, becoming equivalent to the daisy and superdaisy nonperturbative schemes.

We extend the analysis originally conducted in Ref. [61], which studied the complex scalar field model but under the influence of an external magnetic field. Our findings demonstrate that the effects of electric fields on the symmetry properties of this model are not only qualitatively different but also quantitatively distinct compared to the effects of magnetic fields. The methodology we employed to incorporate the electric field allows us to investigate the full range of phase transitions in terms of the electric field and temperatures. In addition to studying the phase transition, we explore the vacuum persistence probability rate (also known as the Schwinger's rate for charged particle creation [62–64]), which is derived from the imaginary part of the thermodynamic potential. We discovered that the vacuum persistence probability rate is enhanced at the critical point of the phase transition. This could potentially serve as a valuable indicator of the critical point in physical systems of interest. To our knowledge, this is the first study of its kind to be conducted in the context of an interacting scalar field theory and across the phase transition.

This work is organized as follows. In Sec. II, we introduce the model and detail its OPT implementation to obtain the effective potential. In Sec. III, the temperature and electric field are introduced through the Schwinger's proper time approach and the scalar field propagator for the model is given. The effective potential at first order in the OPT is explicitly computed. In this same section, we also define and give the result for the vacuum persistent probability rate at the same order of approximation in the OPT scheme. In Sec. IV, we present our main results. The effective potential is studied for different values of temperature and electric field and the phase

behavior of the system is explicitly analyzed. The results for the vacuum persistence probability rate are also presented and studied how it is affected by temperature and for different magnitudes for the electric field. Our conclusions are presented in Sec. V. Four appendices are included where the technical aspects and details of the derivations are presented.

Throughout this paper, we work with the natural units, in which the speed of light, Planck's constant and Boltzmann's constant are all set to 1, $c = \hbar = k_B = 1$. We take the Minkowski metric to be $\text{diag}(+, -, -, -)$.

II. THE MODEL AND THE OPT IMPLEMENTATION

We start by considering the simple case of the self-interacting $\lambda\phi^4$ model, with Lagrangian density given by

$$\mathcal{L} = (D_\mu\phi)^\dagger(D^\mu\phi) - V(\phi\phi^\dagger), \quad (2.1)$$

with a spontaneous symmetry breaking potential ($m^2 > 0$),

$$V(\phi\phi^\dagger) = -m^2\phi\phi^\dagger + \frac{\lambda}{3!}(\phi\phi^\dagger)^2, \quad (2.2)$$

and where $D_\mu = \partial_\mu + iqA_\mu$, with A_μ the Abelian gauge field, here considered as an external background field. As usual, writing the complex field ϕ as $\phi = (\phi_1 + i\phi_2)/\sqrt{2}$. As usual, we can choose to shift the field around the ϕ_1 direction, $\phi_1 \rightarrow \phi_1 + \varphi$, where φ is a background field and which the effective potential is a function of. When φ minimizes the potential, $\varphi \equiv \bar{\varphi}$, it becomes the vacuum expectation value (VEV) of the scalar field, $|\langle\phi_1\rangle| = \bar{\varphi}$ and $|\langle\phi_2\rangle| = 0$. For the tree-level potential, we have from Eq. (2.2) that $\bar{\varphi} \equiv \varphi_0 = \pm\sqrt{6m^2/\lambda}$. Hence, in the symmetry broken phase ϕ_1 is associated with the Higgs field, while ϕ_2 is the Goldstone field. Their Feynman propagators, written in terms of the VEV, is given by

$$D_{\phi_1}(p) = \frac{i}{p^2 + m^2 - \frac{\lambda}{2}\varphi^2 + i\epsilon}, \quad (2.3)$$

$$D_{\phi_2}(p) = \frac{i}{p^2 + m^2 - \frac{\lambda}{6}\varphi^2 + i\epsilon}. \quad (2.4)$$

The OPT implementation starts by interpolating the model (2.1) such that [61]

$$\mathcal{L} \rightarrow \mathcal{L}_\delta = \sum_{i=1}^2 \left\{ \frac{1}{2}(\partial_\mu\phi_i)^2 - \frac{1}{2}\Omega^2\phi_i^2 + \frac{\delta}{2}\eta^2\phi_i^2 - \delta\frac{\lambda}{4!}\phi_i^4 \right\} + \mathcal{L}_{ct,\delta}, \quad (2.5)$$

with $\Omega^2 = -m^2 + \eta^2$ and where $\mathcal{L}_{ct,\delta}$ is the renormalization counterterm contribution to the Lagrangian density. In the interpolated Lagrangian density Eq. (2.5), η is a mass term introduced by the OPT procedure and δ is a bookkeeping (dimensionless) parameter controlling the

order in which the OPT method is carried out. The mass parameter η is obtained at each order of the OPT approximation through a variational principle, which in here we use the principle of minimal sensitivity (PMS) [65]¹. The PMS criterion consists of applying the variational condition to some physical quantity under consideration, which here is taken to be the effective potential, V_{eff} . The PMS criterion then produces an optimal variational mass $\bar{\eta}$, which can then be obtained by the relation

$$\left. \frac{dV_{\text{eff}}}{d\eta} \right|_{\bar{\varphi}, \bar{\eta}, \delta=1} = 0, \quad (2.6)$$

while the VEV for the scalar field, $\bar{\varphi}$, is obtained by minimizing the effective potential,

$$\left. \frac{dV_{\text{eff}}}{d\varphi} \right|_{\bar{\varphi}, \bar{\eta}, \delta=1} = 0. \quad (2.7)$$

In terms of the interpolated model, the propagators given by Eqs. (2.3) and (2.4) now become

$$D_{\phi_1, \delta}(p) = \frac{i}{p^2 - \Omega^2 - \frac{\lambda\delta}{2}\varphi^2 + i\epsilon}, \quad (2.8)$$

$$D_{\phi_2, \delta}(p) = \frac{i}{p^2 - \Omega^2 - \frac{\lambda\delta}{6}\varphi^2 + i\epsilon}. \quad (2.9)$$

The effective potential at first order in the OPT is [61]

$$\begin{aligned} V_{\text{eff}} = & \frac{\Omega^2}{2}\varphi^2 - \delta\frac{\eta^2}{2}\varphi^2 + \delta\frac{\lambda}{4!}\varphi^4 \\ & - i \int_p \ln(p^2 - \Omega^2 + i\epsilon) - \delta\eta^2 \int_p \frac{i}{p^2 - \Omega^2 + i\epsilon} \\ & + \delta\frac{\lambda}{3}\varphi^2 \int_p \frac{i}{p^2 - \Omega^2 + i\epsilon} + \delta\frac{\lambda}{3} \left(\int_p \frac{i}{p^2 - \Omega^2 + i\epsilon} \right)^2, \end{aligned} \quad (2.10)$$

where we have defined $\int_p \equiv \int \frac{d^4p}{(2\pi)^4}$. It is convenient to define an effective scalar propagator in the OPT as

$$D_{\Omega}(p) = \frac{i}{p^2 - \Omega^2 + i\epsilon}, \quad (2.11)$$

and also to express the momentum integrals in the effective potential (2.10), using dimensional regularization in the $\overline{\text{MS}}$ -scheme, as

$$\int_p D_{\Omega}(p) = -\frac{\Omega^2}{(4\pi)^2} \frac{1}{\epsilon} + X(T, \eta), \quad (2.12)$$

$$-i \int_P \ln(-iD_{\Omega}(p)^{-1}) = -\frac{\Omega^4}{2(4\pi)^2} \frac{1}{\epsilon} + Y(\eta), \quad (2.13)$$

where $X(\eta)$ and $Y(\eta)$ are functions of the temperature T and electric field E , and they will be explicitly defined in the next section. In the vacuum, $T = 0$ and $E = 0$, they are given by

$$X(\eta) \Big|_{T=0, E=0} = \frac{\Omega^2}{16\pi^2} \left[\ln\left(\frac{\Omega^2}{M^2}\right) - 1 \right], \quad (2.14)$$

$$Y(\eta) \Big|_{T=0, E=0} = -\frac{\Omega^4}{2(4\pi)^2} \left[\frac{3}{2} - \ln\left(\frac{\Omega^2}{M^2}\right) \right] \quad (2.15)$$

Thus, by adding the appropriate counterterms of renormalization to cancel the ultraviolet divergences in (2.10), the renormalized effective potential in the first-order approximation in the OPT can be generically written as

$$\begin{aligned} V_{\text{eff}}(\varphi, \eta) = & -\frac{m^2}{2}\varphi^2 + (1-\delta)\frac{\eta^2}{2}\varphi^2 + \delta\frac{\lambda}{4!}\varphi^4 + Y(\eta) \\ & + \delta \left\{ -\eta^2 + \frac{\lambda}{3} [\varphi^2 + X(\eta)] \right\} X(\eta), \end{aligned} \quad (2.16)$$

and using the PMS condition (2.6) and from the VEV equation (2.7), we have that

$$\bar{\eta}^2 = \frac{\lambda}{3}\bar{\varphi}^2 + \frac{2\lambda}{3}X(\bar{\eta}), \quad (2.17)$$

$$\bar{\varphi}^2 = 6\frac{m^2}{\lambda} - 4X(\bar{\eta}). \quad (2.18)$$

The effective potential Eq. (2.16), with the Eqs. (2.17) and (2.18) form the basic equations that we need to completely explore the phase structure of the model.

III. THE EFFECTIVE POTENTIAL AT FINITE TEMPERATURE AND IN A CONSTANT ELECTRIC FIELD

Let us now explicitly introduce the effects of temperature and electric field. We start by defining the electric field dependent bosonic propagator, $D_{\Omega}(P, qF)$, by [5, 66, 67]

$$D_{\Omega}(p, qF) = i \int_0^{\infty} ds \frac{e^{-is\Omega^2} e^{ip_{\mu} \left[\frac{\tanh(qFs)}{qF} \right]^{\mu\nu} p_{\nu}}}{\sqrt{\det[\cosh(qFs)]}}, \quad (3.1)$$

where $F_{\mu\nu}$ is the electromagnetic field tensor. Using that the electric and magnetic fields are expressed by $E^i = F^{i0}$ and $B^i = -\sum_{j,k} \varepsilon^{ijk} F^{jk}/2$, we obtain

$$D_{\Omega}(p, qF) = i \int_0^{\infty} ds \frac{e^{-is\Omega^2} e^{i \frac{\tanh(qEs)}{qE} p_{\parallel}^2 + i \frac{\tan(qBs)}{qB} p_{\perp}^2}}{\cosh(qEs) \cos(qBs)}, \quad (3.2)$$

where $p_{\perp}^2 = -(p_1^2 + p_2^2)$ and $p_{\parallel}^2 = p_0^2 - p_3^2$. In the present paper, we work in the case of a non-null constant electric field, $E \neq 0$, and in the absence of a magnetic field, $B = 0$. It is also more convenient to define the expressions in

¹ Note that there are also other possible alternative optimization criteria that can be used, similar to the PMS one [55, 60] and that produces equivalent results. In the present paper we will not consider those alternative procedures.

the Euclidean spacetime. Thus, with $s \rightarrow -i\tau$, $p_0 \rightarrow ip_4$ and $B = 0$, the (Euclidean) scalar propagator becomes

$$D_{\text{Eucl},\Omega}(p, qE) = \int_0^\infty d\tau \frac{e^{-\tau\Omega^2} e^{\left(\frac{\tan(qE\tau)}{qE\tau} p_\parallel^2 + p_\perp^2\right)\tau}}{\cos(qE\tau)}, \quad (3.3)$$

where, in Euclidean spacetime, $p_\parallel^2 = -(p_4^2 + p_3^2)$.

Finite temperature is included through the Matsubara imaginary-time formalism, where $p_4 = \omega_n$, $\omega_n = 2n\pi T$ are the bosonic Matsubara frequencies with $n = 0, \pm 1, \pm 2, \dots$. Here, we also work in the dimensional regularization method to perform the momentum integrals, which are given by

$$\int_p \equiv iT \sum_{p_0=i\omega_n} \left(\frac{e^{\gamma_E} M^2}{4\pi}\right)^\epsilon \int \frac{d^d p}{(2\pi)^d}, \quad (3.4)$$

where M is the regularization scale (in the $\overline{\text{MS}}$ -scheme), γ_E is the Euler-Mascheroni constant and $d = 3 - \epsilon$ in dimensional regularization. This approach will give raise to a thermoelectric contribution, obtained in an analogous way as in the fermionic case [30]. Proceeding now with the evaluation of the renormalized expression for $X(\eta, T, qE)$ and adopting the change of variables $qE\tau \rightarrow t$, we have that

$$\begin{aligned} X(\eta, T, qE) &= \frac{\Omega^2}{16\pi^2} \left[\ln\left(\frac{\Omega^2}{M^2}\right) - 1 \right] \\ &+ \frac{qE}{16\pi^2} \int_0^\infty \frac{dt}{t} e^{-t\frac{\Omega^2}{qE}} \left(\frac{1}{\sin(t)} - \frac{1}{t} \right) \\ &+ \frac{qE}{8\pi^2} \int_0^\infty \frac{dt}{t \sin(t)} e^{-t\frac{\Omega^2}{qE}} \sum_{n=1}^\infty e^{-\frac{n^2 qE}{4T^2 |\tan(t)|}}. \end{aligned} \quad (3.5)$$

Likewise, for $Y(\eta, T, qE)$ we have that

$$\begin{aligned} Y(\eta, T, qE) &= -\frac{\Omega^4}{32\pi^2} \left[\frac{3}{2} - \ln\left(\frac{\Omega^2}{M^2}\right) \right] \\ &+ \frac{(qE)^2}{16\pi^2} \int_0^\infty \frac{dt}{t^2} e^{-t\frac{\Omega^2}{qE}} \left(\frac{1}{\sin(t)} - \frac{1}{t} - \frac{t}{6} \right) \\ &- \frac{(qE)^2}{8\pi^2} \int_0^\infty \frac{dt}{t^2 \sin(t)} e^{-t\frac{\Omega^2}{qE}} \sum_{n=1}^\infty e^{-\frac{n^2 qE}{4T^2 |\tan(t)|}}. \end{aligned} \quad (3.6)$$

It is clear from the functions in the Eqs. (3.5) and (3.6) that there are periodic poles, due to the $\sin(t)$ function, when $t = 0, \pi, 2\pi, 3\pi, \dots$. To deal with these poles, it is convenient to separate the real and imaginary parts of the functions $X(\eta, T, qE)$ and $Y(\eta, T, qE)$ and interpreting the physical results by means of the real contributions. Details of this procedure are given in the Appendices A, B and C. The final result for the real part of the function

$X(\eta, T, qE)$ is given by

$$\begin{aligned} \Re X(\eta, T, qE) &= \frac{\Omega^2}{16\pi^2} \ln\left(\frac{2qE}{M^2}\right) \\ &+ \frac{qE}{8\pi^2} \left\{ -\gamma_E y - \arctan(2y) \right. \\ &+ \left. \sum_{n=1}^\infty \left[\frac{y}{n} - \arctan\left(\frac{2y}{2n+1}\right) \right] \right\} \\ &+ \frac{qE}{8\pi^2} \int_0^\infty \frac{dt}{t \sin(t)} e^{-t\frac{\Omega^2}{qE}} \sum_{n=1}^\infty e^{-\frac{n^2 qE}{4T^2 |\tan(t)|}}, \end{aligned} \quad (3.7)$$

while for $\Re Y(\eta, T, qE)$, we obtain that

$$\begin{aligned} \Re Y(\eta, T, qE) &= \frac{\Omega^4}{32\pi^2} \ln\left(\frac{2qE}{M^2}\right) \\ &- \frac{(qE)^2}{4\pi^2} \left\{ \frac{\gamma_E y^2}{2} + y \arctan(2y) - \frac{1}{4} \ln(1+4y^2) \right. \\ &- \left. \sum_{k=1}^\infty \left[\frac{y^2}{2k} - y \arctan\left(\frac{2y}{2k+1}\right) \right] \right. \\ &+ \left. \frac{2k+1}{4} \ln\left(1 + \frac{y^2}{(2k+1)^2}\right) \right\} \\ &- \frac{(qE)^2}{8\pi^2} \int_0^\infty \frac{dt}{t^2 \sin(t)} e^{-t\frac{\Omega^2}{qE}} \sum_{n=1}^\infty e^{-\frac{n^2 qE}{4T^2 |\tan(t)|}}, \end{aligned} \quad (3.8)$$

where, in the above equations, we have defined $y = \Omega^2/(2qE)$. The thermal integrations in the Eqs. (3.7) and (3.8) are all convergent and they can be integrated numerically in a similar way as it was done in Ref. [25].

The physical renormalized effective potential at first order in the OPT is then given by the real part of V_{eff} ,

$$\begin{aligned} \Re V_{\text{eff}}(\varphi, \eta, T, qE) &= -\frac{m^2}{2} \varphi^2 + \frac{\lambda}{4!} \varphi^4 \\ &- \left(\eta^2 - \frac{\lambda}{3} \varphi^2 \right) \Re X(\eta, T, qE) \\ &+ \frac{\lambda}{3} [\Re X(\eta, T, qE)]^2 - \frac{\lambda}{3} [\Im X(\eta, T, qE)]^2 \\ &+ \Re Y(\eta, T, qE), \end{aligned} \quad (3.9)$$

where the imaginary part of the function $X(\eta, T, qE)$, $\Im X(\eta, T, qE)$, was derived in the App. C and given by Eq. (C9). From Eq. (3.9), the conditions for the PMS, Eq. (2.6), and for the VEV, Eq. (2.7) are then given by

$$\begin{aligned} &\left[-\bar{\eta}^2 + \frac{\lambda}{3} \bar{\varphi}^2 + \frac{2\lambda}{3} \Re X(\bar{\eta}, T, qE) \right] \frac{\partial}{\partial \bar{\eta}} \Re X(\eta, T, qE) \Big|_{\eta=\bar{\eta}} \\ &- \frac{2\lambda}{6} \frac{\partial}{\partial \bar{\eta}} [\Im X(\eta, T, qE)]^2 \Big|_{\eta=\bar{\eta}} = 0, \end{aligned} \quad (3.10)$$

$$\bar{\varphi}^2 = 6 \frac{m^2}{\lambda} - 4 \Re X(\bar{\eta}, T, qE). \quad (3.11)$$

In addition to real part of the effective potential, we also quote the expression for the imaginary part of the

effective potential,

$$\begin{aligned} \Im V_{\text{eff}}(\varphi, \eta, T, qE) &= \Im Y(\eta, qE) \\ &- \left[\eta^2 - \frac{\lambda}{3} \varphi^2 - \frac{2\lambda}{3} \Re X(\eta, T, qE) \right] \Im X(\eta, qE), \end{aligned} \quad (3.12)$$

where the imaginary part of the function Y was derived in the App. C and given by Eq. (C10)². The imaginary part of the effective potential here, which is entirely due to the presence of the background electric field, indicates an instability of the vacuum towards the productions of charged particles due to the electric field. It is known now as the *vacuum persistence probability rate* [68, 69], w , which from Eq. (3.12), we can express it as³

$$w(qE, T) = -2\Im V_{\text{eff}}(\bar{\varphi}, \bar{\eta}, T, qE), \quad (3.13)$$

which for the present problem it is given explicitly as

$$\begin{aligned} w(qE, T) &= -\frac{(qE)^2}{8\pi^3} \text{Li}_2(-e^{-2\pi y}) \Big|_{\eta=\bar{\eta}} \\ &+ \frac{qE}{16\pi^2} \ln(1 + e^{-2\pi y}) \\ &\times \left[\eta^2 - \frac{\lambda}{3} \bar{\varphi}^2 - \frac{2\lambda}{3} \Re X(\eta, T, qE) \right] \Big|_{\eta=\bar{\eta}}, \end{aligned} \quad (3.14)$$

where $\Re X$ is given by Eq. (3.7). It can be checked that in the free (unbroken) theory case, with $\lambda \rightarrow 0$, $\Omega^2 \rightarrow m^2$, $y \rightarrow m^2/(2qE)$, the result given by Eq. (3.14) reproduces the expression for the rate w for the free scalar quantum electrodynamics (QED) case [68],

$$\begin{aligned} w(qE, T) \rightarrow w_{\text{free}}(qE) &= -\frac{(qE)^2}{8\pi^3} \text{Li}_2\left(-e^{-\frac{\pi m^2}{qE}}\right) \\ &= \frac{(qE)^2}{8\pi^3} \sum_{k=1}^{\infty} \frac{(-1)^{k-1} e^{-\frac{\pi m^2 k}{qE}}}{k^2}. \end{aligned} \quad (3.15)$$

Note that the result for the free scalar QED is independent of the temperature. In this way, we can see that the OPT at first order includes thermal and interaction dependent corrections to the imaginary part of the effective potential (and hence to w), with the optimum mass parameter $\bar{\eta}$ determined by the PMS condition Eq. (3.10) and with $\bar{\varphi}$ given by Eq. (3.11).

Before we close this Section, it is worth to remark that the imaginary part of the effective potential given by Eq. (3.12) should not be confused with the situation

when the finite temperature effective potential can become imaginary, in a symmetry broken theory and in perturbation theory, for some values of the background field. In that case, the imaginary part of the effective potential can be interpreted as a decay width of the localized quantum state, used to perturbatively evaluate the effective potential, to the true vacuum state [70]. As far as the derivation of the effective potential is concerned, we do not have such issues of imaginary terms as plagued the perturbative calculation. In particular, the OPT effective mass squared appearing in the propagator Eq. (2.11), Ω^2 , remains always positive definite, with $\bar{\eta}^2 \geq m^2$. This is a result known from previous studies in the context of the OPT (see, in particular the Refs. [57, 61]). The same remains true in the present study, as we explicitly verify in the next Section. In particular, it is important to also remark that the OPT preserves the Goldstone theorem, as demonstrated in Refs. [57, 61].

IV. NUMERICAL RESULTS

In this Section, we explore the numerical results of the model. Let us start by studying the effective potential Eq. (3.9) as a function of the background field and for different values of temperature and electric field. Our results show that there is a threshold value for the electric field below which the phase transition is first order, while above it the transition becomes second order. In Fig. 1 we have used a representative choice of model parameters, e.g., $\lambda = 1$ and $m = 0.1M$ (we express all dimensional quantities in terms of the regularization scale M). This is a choice of parameters where the results start becoming more sensitive to the effects of the electric field and one that allows us to compare the results in the absence of E more easily.

We express our results in terms of the reduced effective potential, $\Delta V_{\text{eff}} = V_{\text{eff}}(\varphi, \bar{\eta}, T, qE) - V_{\text{eff}}(0, \bar{\eta}_0, T, qE)$, where $\bar{\eta}_0$ is the optimal value of η when evaluated at $\varphi = 0$. In Fig. 1, we show the reduced effective potential for different values of temperature around the critical value. The transition pattern shown in Fig. 1(a) is that of a typical first-order phase transition. The electric field considered in that case was $E = 0$. By increasing the electric field, eventually above a threshold value the transition becomes second-order. This is illustrated in Fig. 1(b), which shows a typical second-order phase transition where the VEV decreases as the temperature increases and becomes zero at the critical temperature. The electric field considered in this case was $qE = 0.2M^2$. The critical temperature for the first-order phase transition seen in the case shown in Fig. 1(a) is found to be given by $T_c \simeq 0.426725M$, while for the case of the second-order phase transition seen in Fig. 1(b) is $T_c \simeq 0.424180M$.

² Issues concerning the derivation of the imaginary part of the loop diagrams in a thermal bath are discussed in the App. C.

³ The vacuum persistence probability itself is $P_{\text{vac}}(t) = e^{-w\mathcal{V}t}$, where \mathcal{V} is the spatial volume of the system and w is the rate of vacuum decay per unit volume.

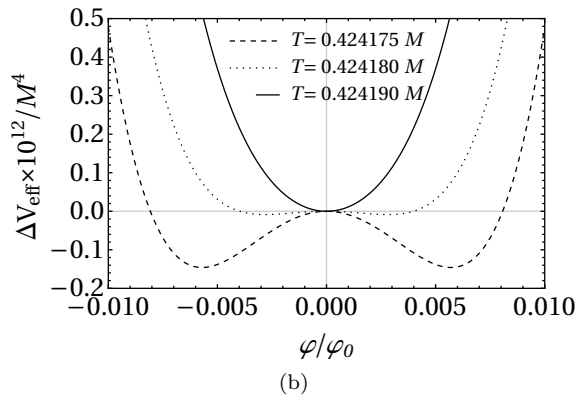
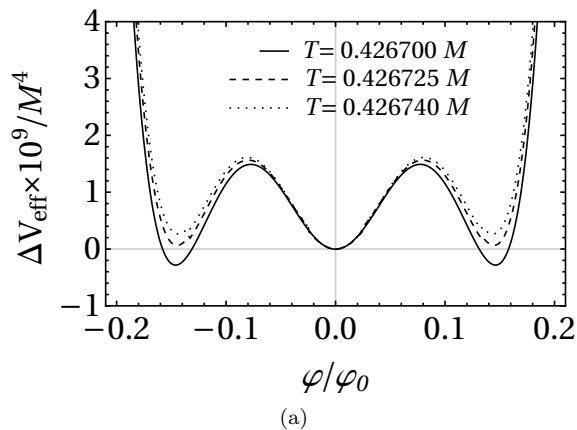


FIG. 1. Reduced effective potential $\Delta V_{\text{eff}}(qE, T, \bar{\eta}, \varphi)$ as a function of φ/φ_0 for different values of temperature T/M for $qE = 0$ (panel a) and for $qE = 0.2M^2$ (panel b). The model parameters chosen are $\lambda = 1$ and $m = 0.1M$.

Despite the different transition patterns and changes in the electric field, the critical temperature for phase transition remains relatively constant, indicating a very weak dependence on the external electric field. This intriguing result is further explored below. Previous studies of the same model in the absence of electric fields ($E = 0$) [71] also found a first-order phase transition. In Ref. [71], the authors investigated the phase transition behavior of the complex scalar field using the ring diagram approximation. Our results align with this finding, as we also observe a first-order phase transition up to the threshold value of the electric field within the context of the OPT. While not explicitly shown here, we have explored the phase transition for different parameter values and found that the threshold value for the electric field depends on these choices. For example, with $\lambda = 2$ and $m = M$, we obtain $qE_{\text{threshold}} \simeq 0.08M^2$, while for $\lambda = 1$ and $m = M$ we find that $qE_{\text{threshold}} \gtrsim 0.048M^2$. In general, increasing the self-coupling tends to increase the threshold value for the electric field at which the phase transition changes from first-order to second-order.

It is also relevant to look at the behavior of the VEV

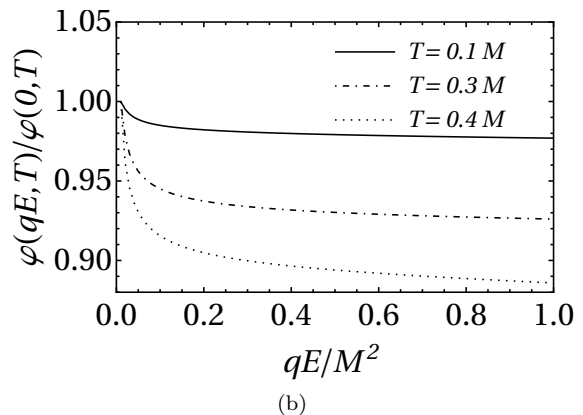
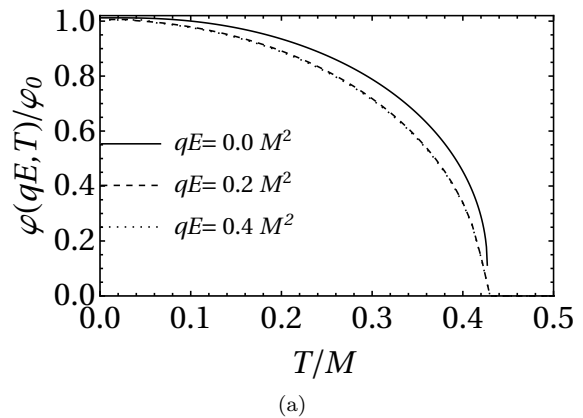


FIG. 2. The VEV as a function of the temperature (panel a) and as a function of the electric field. The model parameters chosen are $\lambda = 1$ and $m = 0.1M$.

as a function of temperature and electric field. In Fig. 2 we show the normalized VEV $\bar{\varphi}/\varphi_0$, where $\bar{\varphi} \equiv \varphi(qE, T)$ and $\varphi_0^2 = 6m^2/\lambda$, which is shown as a function of the temperature and for different values of the external electric field (panel a) and as a function of the electric field and different values of the temperature (panel b). In Fig. 2(a), we can see that at $qE = 0$ we have the usual symmetry restoration pattern, e.g. as previously observed in [61], in which the $\bar{\varphi}/\varphi_0$ decreases as a function of T . Note also the discontinuity of the VEV close to the critical temperature, indicating a first-order phase transition, which persists up to the threshold value for the electric field discussed above. Above the threshold value for E , the VEV always decreases in a smooth way, vanishing at the critical point, as expected for a second-order phase transition. Note also that for higher values of qE the magnitude of $\bar{\varphi}/\varphi_0$ at intermediate values of temperature in between $T = 0$ and $T = T_c$ cause a more prominent change of the VEV. This behavior is also seen more clearly in Fig. 2(b), where we show the behavior of the VEV as a function of the electric field. In all cases, we find that the critical temperature, T_c , can be well

approximately by

$$T_c^2 \simeq \frac{18m^2}{\lambda}, \quad (4.1)$$

which, for the model parameters chosen, it gives $T_c/M \simeq 0.424180$, in agreement with the critical temperature obtained in Fig. 1, when studying directly the effective potential. As shown in the App. D, this result turns out to be a very good approximation, with T_c presenting a very weak dependence on the electric field, even for very strong fields, $qE \gg m^2$.

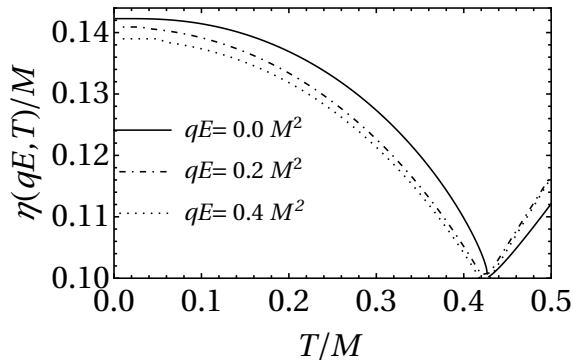


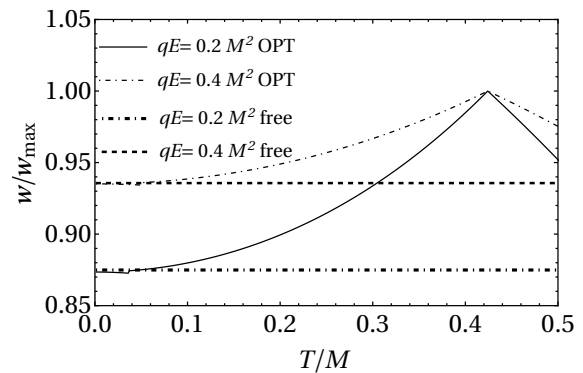
FIG. 3. The optimum OPT mass parameter $\bar{\eta}(qE, T)$ as a function of the temperature and for different values for the electric field.

It is also useful to look at how the optimum OPT mass parameter $\bar{\eta}$ changes with the temperature and with the magnitude of the electric field. This is shown in the Fig. 3. For $qE = 0$, starting from $T = 0$ up to $T = T_c$, we see the usual decrease of $\bar{\eta}$ (see, e.g., Refs. [57, 61]) until it reaches the value $\bar{\eta} = m$ at $T = T_c$. For higher values of qE , the values of $\bar{\eta}$ have a similar behavior. For $T > T_c$, $\bar{\eta}$ starts to grow with the temperature and the electric field, showing an inverse behavior of the one seen in the region with $T < T_c$.

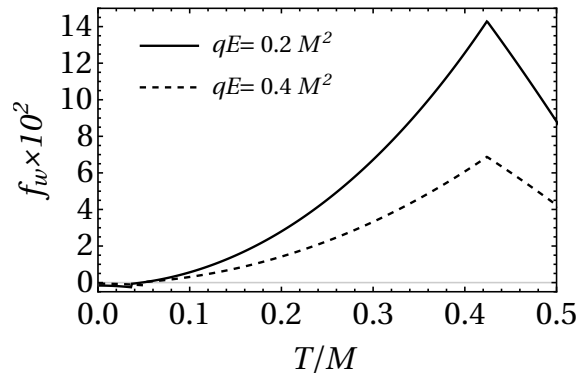
Finally, let us now investigate the temperature and electric field dependence for the vacuum persistence probability rate, given by Eq. (3.14). In Fig. 4(a) we show the results for the interaction theory (curves labeled by OPT) and which are given by Eq. (3.14). These results are also compared to the free theory one, given by Eq. (3.15) (curves labeled by free). Two representative values for the electric field are used. In Fig. 4(b) we also show the fractional difference for the rates, f_w , defined by

$$f_w = \frac{w_{\text{OPT}} - w_{\text{free}}}{w_{\text{free}}}. \quad (4.2)$$

From the results shown in Fig. (4) we can see that the rate w peaks exactly at the critical temperature (which



(a)



(b)

FIG. 4. The vacuum persistence probability rate as a function of the temperature for the interaction theory (curves labeled by OPT) and for the free theory (panel a) and for the fractional difference, defined in Eq. (4.2) (panel b).

for the model parameters considered, is given by $T_c/M \simeq 0.424180$). For $T \ll T_c$ and for $T \gg T_c$, the rate tends to the free scalar QED result Eq. (3.15). In particular, considering the expression for the rate Eq. (3.14) at $T = T_c$ and using the results from App. D, we obtain that at the critical temperature,

$$w(qE, T_c) \simeq \frac{(qE)^2}{96\pi}, \quad (4.3)$$

which, surprisingly, does not depend on the coupling constant, even though away from the critical temperature, there is an explicit dependence on the interaction in Eq. (3.14). We can also obtain approximate results in the regions $T \ll T_c$ and $T \gg T_c$. By considering $T \ll T_c$, from Eqs. (3.10) and (3.11) we find that $\bar{\eta}^2 - 2m^2 \approx 0$, where we have used that $\bar{\varphi} \simeq \varphi_0$ for $T \ll T_c$ (see, e.g., Fig. 2). Hence, $\Omega^2 \approx m^2$ and $2\pi\gamma \approx \pi m^2/(qE)$. Also, the PMS equation (3.10) implies that the last term on the right-hand side in Eq. (3.14) is negligible. As a consequence, we can conclude that $w_{\text{OPT}} \approx w_{\text{free}}$. This is consistent with the result seen in Fig. 4 in the low-temperature regime. On the other hand, for $T \gg T_c$, we are in the symmetry restored phase, $\bar{\varphi} = 0$. The optimum OPT parameter $\bar{\eta}$ in this region

grows proportional to the temperature, $\bar{\eta} \propto T$, as seen from Fig. 3, for $T > T_c$, and where the effect of the electric field is to further enhance $\bar{\eta}$. In this high temperature symmetry restored region, with also $T \gg m$, then we have the y variable in Eq. (3.14) is much larger than $m^2/(2qE)$ and the rate is exponentially suppressed when compared to the free theory result Eq. (3.15). Hence, $w_{\text{OPT}} \rightarrow 0$ in this high temperature regime. In summary, we can conclude that the rate w is such that $w_{\text{free}} \lesssim w \lesssim (qE)^2/(96\pi)$ for $T \leq T_c$ (symmetry broken region) and $0 \lesssim w \lesssim (qE)^2/(96\pi)$ for $T \geq T_c$ (in the symmetry restored region). The maximum value attained by the rate is always $w_{\text{max}} \approx (qE)^2/(96\pi)$, which happens at $T = T_c$. Again, this overall behavior is confirmed by our numerical results shown in Fig. 4.

V. CONCLUSIONS

We investigated the phase transition for symmetry restoration in a charged scalar field theory, considering the combined effects of temperature and an external constant electric field. Our study utilized the nonperturbative method of the optimized perturbation theory (OPT) in its first nontrivial order. We derived the effective potential for the model that explicitly incorporates the temperature and electric field dependence. To achieve this, we employed the Schwinger's proper time scalar propagator in the presence of a background electromagnetic field. Our results provide valuable insights into the interplay between temperature and electric fields in influencing the phase behavior of this system.

We numerically investigated the symmetry restoration of the model starting from the broken phase at low temperatures. We found that for weak electric fields, $qE \lesssim m^2$, the transition is first-order. As the electric field increases, the transition becomes second-order. We observed that increasing the quartic self-coupling constant lowers the threshold value of the electric field at which the transition changes from first to second order. Additionally, we studied the behavior of the critical temperature for phase transition as a function of the electric field. Both numerically and analytically, we discovered a surprisingly weak dependence on the electric field, which holds for both types of phase transitions. This behavior is significantly different from the strong dependence of the critical temperature on the magnetic field B observed in previous studies (like in Ref. [61]) using the OPT at a similar order.

In addition to studying how the phase structure of the model changes with the applied external electric field, we have also obtained the vacuum persistence probability rate, which is defined in terms of the imaginary part of the effective potential. We have shown, both numerically and analytically, that at the transition point, the rate reaches a maximum value. The maximum value found for the rate is $w_{\text{max}} \simeq (qE)^2/(96\pi)$ which is independent of the coupling constant of the model. We have also

seen that for the symmetry broken region, $0 \leq T \leq T_c$, the rate has a lower bound value set by the rate of the free QED theory, given by Eq. (3.15) and as the temperature increases, it increases until reaching the value w_{max} at $T = T_c$. In the symmetry restored phase, the rate decreases exponentially, vanishing asymptotically for $T \gg T_c$.

The results presented in this paper could have significant implications for various fields, such as QCD topology in the presence of extreme electromagnetic fields. In these scenarios, the coupling between axions and photons can be calculated using effective models and compared with recent lattice simulations [73]. Understanding the behavior of meson masses as functions of magnetic fields has been a subject of interest, with various effective QCD models and lattice simulations exploring this topic [74, 75]. Ongoing calculations are investigating the effects of strong electric fields on meson masses and will be reported in future publications.

Appendix A: Evaluation of pure electric part of

$$X(\eta, T = 0, qE)$$

In order to obtain the pure electric field contribution for the function $X(\eta, T, qE)$, given by Eq. (3.5), and at $T = 0$, we can use the analytic continuation $qB \rightarrow -iqE$ [25, 26, 30] in the pure magnetic contribution of the function $X(qB, \Omega)$ given by the Eq. (3.23) derived in Ref. [61],

$$\begin{aligned} X(qB, \Omega) &= \frac{qB}{8\pi^2} \ln \left[\Gamma \left(\frac{\Omega^2}{2qB} + \frac{1}{2} \right) \right] - \frac{qB}{16\pi^2} \ln(2\pi) \\ &\quad - \frac{\Omega^2}{16\pi^2} \ln \left(\frac{M^2}{2qB} \right). \end{aligned} \quad (\text{A1})$$

In the first term in Eq. (A1), we can use the identity [25]

$$\ln \Gamma(x) = -\gamma_E x + \ln(x) + \sum_{k=1}^{\infty} \left[\frac{x}{k} - \ln \left(1 + \frac{x}{k} \right) \right], \quad (\text{A2})$$

where $\gamma_E = 0.57721$ is the Euler-Mascheroni constant. We can change $x \rightarrow iy + \frac{1}{2}$, where $y = \frac{\Omega^2}{2qE}$. Hence, we find that

$$\begin{aligned} \ln \Gamma \left(iy + \frac{1}{2} \right) &= -\gamma_E \left(iy + \frac{1}{2} \right) - \ln \left(iy + \frac{1}{2} \right) \\ &\quad + \sum_{k=1}^{\infty} \left[\frac{iy + \frac{1}{2}}{k} - \ln \left(1 + \frac{iy + \frac{1}{2}}{k} \right) \right] \\ &= -\gamma_E iy - \frac{\gamma_E}{2} - \ln \left(iy + \frac{1}{2} \right) \\ &\quad + \sum_{k=1}^{\infty} \left[\frac{iy}{k} + \frac{1}{2k} - \ln \left(1 + \frac{iy}{k} + \frac{1}{2k} \right) \right]. \end{aligned} \quad (\text{A3})$$

Now, using $z = a + ib$ and that $\ln(z)$ is given by

$$\ln(z) = \ln|a^2 + b^2| + i\theta, \quad \theta = \arctan\left(\frac{b}{a}\right), \quad (\text{A4})$$

we obtain that

$$\ln\left(iy + \frac{1}{2}\right) = \ln\left|y^2 + \frac{1}{4}\right| + i\theta, \quad (\text{A5})$$

$$\ln\left(\frac{iy}{k} + \frac{1}{2k} + 1\right) = \ln\left|\frac{y^2}{k^2} + \left(\frac{1}{2k} + 1\right)^2\right| + i\theta_k, \quad (\text{A6})$$

where $\theta = \arctan(2y)$ and $\theta_k = \arctan[2y/(2k+1)]$. From these results, we can separate $\ln\Gamma\left(iy + \frac{1}{2}\right)$ in its real and imaginary parts as

$$\begin{aligned} \Re\left[\ln\Gamma\left(iy + \frac{1}{2}\right)\right] &= -\frac{\gamma_E}{2} - \ln\left|y^2 + \frac{1}{4}\right| \\ &+ \sum_{k=1}^{\infty} \left[\frac{1}{2k} - \ln\left|\frac{y^2}{k^2} + \left(\frac{1}{2k} + 1\right)^2\right| \right], \end{aligned} \quad (\text{A7})$$

$$\begin{aligned} \Im\left[\ln\Gamma\left(-iy + \frac{1}{2}\right)\right] &= -\gamma_E y - \arctan(2y) \\ &+ \sum_{k=1}^{\infty} \left[\frac{y}{k} - \arctan\left(\frac{-2y}{2k+1}\right) \right]. \end{aligned} \quad (\text{A8})$$

Hence, the first term of Eq. (A1), in the analytical continuation $qB \rightarrow -iqE$, is given by

$$\begin{aligned} \frac{-iqE}{8\pi^2} i\Im\left[\ln\Gamma\left(-iy + \frac{1}{2}\right)\right] &= \frac{qE}{8\pi^2} \left\{ -\gamma_E y - \arctan(2y) \right. \\ &\left. + \sum_{k=1}^{\infty} \left[\frac{y}{k} - \arctan\left(\frac{-2y}{2k+1}\right) \right] \right\}, \end{aligned} \quad (\text{A9})$$

while the remaining terms in Eq. (A1) are trivial to obtain the analytical continuation. Thus, the pure electric field contribution of Eq. (A1) is found to be given by

$$\begin{aligned} \Re X(\eta, T=0, qE) &= \frac{qE}{8\pi^2} \left\{ -\gamma_E y - \arctan(2y) + \right. \\ &\left. \sum_{n=1}^{\infty} \left[\frac{y}{n} - \arctan\left(\frac{2y}{2n+1}\right) \right] \right\} + \frac{\Omega^2}{16\pi^2} \ln\left(\frac{2qE}{M^2}\right). \end{aligned} \quad (\text{A10})$$

Appendix B: Evaluation of pure electric part of $Y(\eta, T=0, qE)$

Let us now apply the same procedure as done in App. A to find the pure electric field contribution for the function $Y(\eta, T, qE)$, given by Eq. (3.6), and at $T=0$. But first

one notices that the renormalized functions X and Y are related to each other,

$$\frac{\partial Y}{\partial \Omega^2} = X, \quad (\text{B1})$$

which can be easily verified from their general expressions, given by Eqs. (2.12) and (2.13). Therefore, it is straightforward to obtain $Y(\eta, qE, T=0)$ by

$$\int d\Omega^2 X(qE, \Omega, T=0) = Y(qE, \Omega, T=0), \quad (\text{B2})$$

up to an irrelevant constant to the effective potential. Then, by simple integration, one obtains

$$\begin{aligned} \Re Y(qE, T=0, \Omega) &= \frac{\Omega^4}{32\pi^2} \ln\left(\frac{2qE}{M^2}\right) \\ &- \frac{(qE)^2}{4\pi^2} \left\{ \frac{\gamma_E y^2}{2} + y \arctan(2y) - \frac{1}{4} \ln(1+4y^2) \right. \\ &- \sum_{k=1}^{\infty} \left[\frac{y^2}{2k} - y \arctan\left(\frac{2y}{2k+1}\right) \right. \\ &\left. \left. + \frac{2k+1}{4} \ln\left(1 + \frac{4y^2}{(2k+1)^2}\right) \right] \right\}, \end{aligned} \quad (\text{B3})$$

which is the pure electric field part of Eq. (3.8).

Appendix C: Imaginary part of functions $X(\eta, T, qE)$ and $Y(\eta, T, qE)$

By using the same techniques applied in Ref.[25], we can show that imaginary contribution of the thermo-electric part of the functions $X(\eta, qE, T)$ and $Y(\eta, T, qE)$ are zero. Writing $X(\eta, T, qE)$ in terms of a $T=0$ and $T \neq 0$ terms,

$$X(\eta, T, qE) = X_{qE}(\eta, qE) + X_{qE, T}(\eta, T, qE), \quad (\text{C1})$$

where $Y_{qE}(\eta, qE)$ is the pure electric part and $Y_{qE, T}(\eta, T, qE)$ is thermo-electric contribution, given by

$$\begin{aligned} X_{qE, T}(\eta, T, qE) &= \frac{(qE)^2}{8\pi^2} \int_0^{\infty} \frac{dt}{t \sin(t)} e^{-t \frac{\Omega^2}{qE}} \\ &\times \sum_{n=1}^{\infty} e^{-\frac{n^2 qE}{4T^2 |\tan(t)|}} \\ &= \frac{(qE)^2}{8\pi^2} \int_0^{\infty} \frac{dt \cot(t)}{t \cos(t)} e^{-t \frac{\Omega^2}{qE}} \\ &\times \sum_{n=1}^{\infty} e^{-\frac{n^2 qE}{4T^2 |\tan(t)|}}, \end{aligned} \quad (\text{C2})$$

where we have appropriately rewritten the terms in order to use the following identity

$$\cot(t) = \frac{1}{t} + \sum_{k=1}^{\infty} \left(\frac{1}{t - k\pi} + \frac{1}{t + k\pi} \right). \quad (\text{C3})$$

The only term that contributes to the imaginary part of $X_{qE,T}(\eta, T, qE)$ is given by

$$\begin{aligned} \Im X_{qE,T}(\eta, T, qE) &= \frac{(qE)^2}{8\pi^2} \int_0^\infty \frac{dt}{t \cos(t)} e^{-t \frac{\Omega^2}{qE}} \\ &\times \sum_{n=1}^\infty e^{-\frac{n^2 qE}{4T^2 |\tan(t)|}} \sum_{k=1}^\infty \delta(t - k\pi) \rightarrow 0, \end{aligned} \quad (\text{C4})$$

where we have used $\lim_{\epsilon \rightarrow 0} \frac{1}{x \pm i\epsilon} = \text{P.V.} \frac{1}{x} \mp i\pi \delta(x)$. Then, in order to obtain the imaginary part of both functions, we can use the result obtained in the magnetic field system, obtained in Ref. [61], and using again the duality relation $qB \rightarrow -iqE$, which gives

$$\begin{aligned} X(\eta, qE) &= \frac{-iqE}{8\pi^2} \ln \Gamma \left(iy + \frac{1}{2} \right) + \frac{iqE}{16\pi^2} \ln(2\pi) \\ &- \frac{\Omega^2}{16\pi^2} \ln \left(\frac{M^2}{-iqE} \right). \end{aligned} \quad (\text{C5})$$

Then, it is now easy to evaluate $\Im X(\eta, qE)$, which is given by

$$\Im X(\eta, qE) = -\frac{qE}{8\pi^2} \left\{ \Re \left[\ln \Gamma \left(iy + \frac{1}{2} \right) \right] - \frac{\ln(2\pi)}{2} + \frac{y\pi}{2} \right\}. \quad (\text{C6})$$

By also using the identity $\Re[\ln(iy + \frac{1}{2})] = [\ln \Gamma(iy + \frac{1}{2}) + \ln \Gamma(-iy + \frac{1}{2})] / 2$, we can work on the first term of the right-hand side of the previous expression. Then, by also using that

$$\frac{\ln \Gamma |iy + \frac{1}{2}|^2}{2} = \frac{1}{2} \ln \left(\frac{\pi}{\cosh(\pi y)} \right), \quad (\text{C7})$$

which is obtained by analytic continuation to the complex plane of the expression $\Gamma[x]\Gamma[1-x] = \pi(\sin(\pi x))^{-1}$, after some algebra, we obtain

$$\begin{aligned} \frac{\ln \Gamma |iy + \frac{1}{2}|^2}{2} &= \frac{\ln \pi}{2} - \frac{1}{2} \ln(e^{\pi y}) - \frac{1}{2} \ln \left(\frac{1 + e^{-2\pi y}}{2} \right) \\ &= \frac{\ln(2\pi)}{2} - \frac{y\pi}{2} - \frac{1}{2} \sum_{k=1}^\infty \frac{(-1)^k e^{-2\pi y k}}{k} \\ &= \frac{\ln(2\pi)}{2} - \frac{y\pi}{2} - \frac{1}{2} \ln(1 + e^{-2\pi y}). \end{aligned} \quad (\text{C8})$$

Using these results in Eq. (C5), we obtain

$$\Im X(\eta, qE) = \frac{qE}{16\pi^2} \ln(1 + e^{-2\pi y}). \quad (\text{C9})$$

By integration in Ω^2 , like in Eq. (B2), we then obtain

$$\Im[Y(\eta, qE)] = \frac{(qE)^2}{16\pi^3} \text{Li}_2(-e^{-2\pi y}), \quad (\text{C10})$$

where we have again neglected an irrelevant constant factor when obtaining (C10) and that can always be subtracted from the effective potential and $\text{Li}_2(x)$, is the Polylogarithm function, $\text{Li}_2(x) = \sum_{k=1}^\infty x^k/k^2$. The above results show that the imaginary parts of both the functions X and Y are not explicitly dependent on the temperature.

It is important to remark here that, in the context of electric fields, there is no clear consensus on the form or even the existence of one-loop thermal contributions for the imaginary part of the effective potential. These possible thermal effects will contribute to the vacuum persistence probability rate [76–82]. In particular, the worldline method has been used to derive these thermal contributions to the vacuum persistence probability rate [83–85]. These studies have shown that the thermal contributions become relevant (compared to the $T = 0$ result) at a threshold temperature $T_{CW} = \frac{eE}{2\Omega}$. Below T_{CW} the thermal bath's energy is insufficient to create a charged particle-antiparticle pair accelerated by the electric field over their Compton wavelength. In this regime, thermal effects are negligible, and charged particle-antiparticle pairs are produced only through quantum processes. All the numerical results presented in Sec. IV focus on the region where these possible thermal contributions to the effective potential and vacuum persistence probability rate can be ignored, i.e., we focus on the regime $T < T_{CW}$.

Appendix D: Independence of the critical temperature with the electric fields

Let us now demonstrate that the critical temperature is indeed very weakly dependent on the electric field. To evaluate the critical temperature, we consider the situation where $\bar{\varphi} = 0$ and, therefore, $\Omega = 0$, since $\bar{\eta}^2 = m^2$ and as demonstrated in Ref. [61]. This is an approximation of Eq. (3.10), since we are considering the second contribution very small. The second contribution term in Eq. (3.10), and that involves $\Im X$, can be neglected, which is justified by the numerical results we have obtained in Sec. IV, and implies that $T_c(qE) \approx T_c(0)$. Then,

$$\frac{6m^2}{\lambda} - 4X(T_c, qE, \bar{\eta}) \approx 0, \quad (\text{D1})$$

where

$$X(T_c, qE, \bar{\eta}) = \frac{qE}{8\pi^2} \int_0^\infty \frac{dt}{t \sin(t)} \sum_{n=1}^\infty e^{-\frac{n^2 qE}{4T_c^2 |\tan(t)|}}. \quad (\text{D2})$$

From a change of variables, we can also write Eq. (D2) as

$$X(T_c, qE, \eta) = \sum_{n=1}^{\infty} \frac{qE}{8\pi^2} \int_0^{\infty} \frac{d\tau}{\sqrt{1+\tau^2}} e^{-\frac{n^2 qE}{4T_c^2} \tau} \times \frac{4}{\pi} \sum_{k=0}^{\infty} \left[\frac{(-1)^k (2k+1)}{(2k+1)^2 - \left(\frac{\pi}{2} \tan^{-1} \tau\right)^2} \right]. \quad (\text{D3})$$

Now, we can make use of the identity [72],

$$\sum_{k=0}^{\infty} \left[\frac{(-1)^k (2k+1)}{(2k+1)^2 - a^2} \right] = \frac{\pi}{4} \sec\left(\frac{\pi a}{2}\right), \quad (\text{D4})$$

as well as the property $\sec(\tan^{-1} \tau) = \sqrt{1+\tau^2}$. Then, applying these results in Eq. (D3), we obtain

$$X(T_c, qE, \eta) = \frac{qE}{8\pi^2} \sum_{n=1}^{\infty} \int_0^{\infty} d\tau e^{-\frac{n^2 qE}{4T_c^2} \tau}, \quad (\text{D5})$$

which can be easily integrated, resulting in

$$X(T_c, qE, \bar{\eta}) = \frac{T_c^2}{12}, \quad (\text{D6})$$

which is exactly the same result as obtained in Ref. [61] in the case of $qE = 0$. When we apply the last result in

Eq. (D1), we obtain

$$T_c^2 = \frac{18m^2}{\lambda}, \quad (\text{D7})$$

and which is in full agreement with the numerical results obtained in Sec. IV.

ACKNOWLEDGMENTS

This work was partially supported by Conselho Nacional de Desenvolvimento Científico e Tecnológico (CNPq), 312032/2023-4 (R.L.S.F.), 304518/2019-0 (S.S.A.), 307286/2021-5 (R.O.R.); Fundação Carlos Chagas Filho de Amparo à Pesquisa do Estado do Rio de Janeiro (FAPERJ), Grant No. SEI-260003/019544/2022 (W.R.T), Grant No. E-26/201.150/2021 (R.O.R.); Fundação de Amparo à Pesquisa do Estado do Rio Grande do Sul (FAPERGS), Grants Nos. 19/2551-0000690-0 and 19/2551-0001948-3 (R.L.S.F.); The work is also part of the project Instituto Nacional de Ciência e Tecnologia - Física Nuclear e Aplicações (INCT - FNA), Grant No. 464898/2014-5.

-
- [1] N. Goldenfeld, Lectures on Phase Transitions and The Renormalization Group, Frontiers in Physics, Vol. 85 (Addison-Wesley, NY, 1992).
- [2] A. D. Linde, Phase Transitions in Gauge Theories and Cosmology, Rept. Prog. Phys. **42**, 389 (1979) doi:10.1088/0034-4885/42/3/001
- [3] V. A. Miransky and I. A. Shovkovy, Quantum field theory in a magnetic field: From quantum chromodynamics to graphene and Dirac semimetals, Phys. Rept. **576**, 1-209 (2015) doi:10.1016/j.physrep.2015.02.003 [arXiv:1503.00732 [hep-ph]].
- [4] J. O. Andersen, W. R. Naylor and A. Tranberg, Phase diagram of QCD in a magnetic field: A review, Rev. Mod. Phys. **88**, 025001 (2016) doi:10.1103/RevModPhys.88.025001 [arXiv:1411.7176 [hep-ph]].
- [5] K. Hattori, K. Itakura and S. Ozaki, Strong-field physics in QED and QCD: From fundamentals to applications, Prog. Part. Nucl. Phys. **133**, 104068 (2023) doi:10.1016/j.pnpnp.2023.104068 [arXiv:2305.03865 [hep-ph]].
- [6] G. Endrodi, QCD with background electromagnetic fields on the lattice: a review, [arXiv:2406.19780 [hep-lat]].
- [7] D. Allor, T. D. Cohen and D. A. McGady, The Schwinger mechanism and graphene, Phys. Rev. D **78**, 096009 (2008) doi:10.1103/PhysRevD.78.096009 [arXiv:0708.1471 [cond-mat.mes-hall]].
- [8] I. Akal, R. Egger, C. Müller and S. Villalba-Chávez, Simulating dynamically assisted production of Dirac pairs in gapped graphene monolayers, Phys. Rev. D **99**, no.1, 016025 (2019) doi:10.1103/PhysRevD.99.016025 [arXiv:1812.03846 [cond-mat.mes-hall]].
- [9] W. T. Deng and X. G. Huang, Event-by-event generation of electromagnetic fields in heavy-ion collisions, Phys. Rev. C **85**, 044907 (2012) doi:10.1103/PhysRevC.85.044907 [arXiv:1201.5108 [nucl-th]].
- [10] A. Bzdak and V. Skokov, Event-by-event fluctuations of magnetic and electric fields in heavy ion collisions, Phys. Lett. B **710**, 171-174 (2012) doi:10.1016/j.physletb.2012.02.065 [arXiv:1111.1949 [hep-ph]].
- [11] J. Błoczyński, X. G. Huang, X. Zhang and J. Liao, Azimuthally fluctuating magnetic field and its impacts on observables in heavy-ion collisions, Phys. Lett. B **718**, 1529-1535 (2013) doi:10.1016/j.physletb.2012.12.030 [arXiv:1209.6594 [nucl-th]].
- [12] J. Błoczyński, X. G. Huang, X. Zhang and J. Liao, Charge-dependent azimuthal correlations from AuAu to UU collisions, Nucl. Phys. A **939**, 85-100 (2015) doi:10.1016/j.nuclphysa.2015.03.012 [arXiv:1311.5451 [nucl-th]].
- [13] Y. Hirono, M. Hongo and T. Hirano, Estimation of electric conductivity of the quark gluon plasma via asymmetric heavy-ion collisions, Phys. Rev. C **90**,

- no.2, 021903 (2014) doi:10.1103/PhysRevC.90.021903 [arXiv:1211.1114 [nucl-th]].
- [14] V. Voronyuk, V. D. Toneev, S. A. Voloshin and W. Cassing, Charge-dependent directed flow in asymmetric nuclear collisions, *Phys. Rev. C* **90**, no.6, 064903 (2014) doi:10.1103/PhysRevC.90.064903 [arXiv:1410.1402 [nucl-th]].
- [15] W. T. Deng and X. G. Huang, Electric fields and chiral magnetic effect in Cu+Au collisions, *Phys. Lett. B* **742**, 296-302 (2015) doi:10.1016/j.physletb.2015.01.050 [arXiv:1411.2733 [nucl-th]].
- [16] X. G. Huang, Electromagnetic fields and anomalous transports in heavy-ion collisions — A pedagogical review, *Rept. Prog. Phys.* **79**, no.7, 076302 (2016) doi:10.1088/0034-4885/79/7/076302 [arXiv:1509.04073 [nucl-th]].
- [17] A. K. Panda, P. Bagchi, H. Mishra and V. Roy, Electromagnetic fields in low-energy heavy-ion collisions with baryon stopping, *Phys. Rev. C* **110**, no.2, 024902 (2024) doi:10.1103/PhysRevC.110.024902 [arXiv:2404.08431 [nucl-th]].
- [18] H. Taya, T. Nishimura and A. Ohnishi, Estimation of electric field in intermediate-energy heavy-ion collisions, *Phys. Rev. C* **110**, no.1, 014901 (2024) doi:10.1103/PhysRevC.110.014901 [arXiv:2402.17136 [hep-ph]].
- [19] K. Fukushima, D. E. Kharzeev and H. J. Warringa, The Chiral Magnetic Effect, *Phys. Rev. D* **78**, 074033 (2008) doi:10.1103/PhysRevD.78.074033 [arXiv:0808.3382 [hep-ph]].
- [20] D. T. Son and A. R. Zhitnitsky, Quantum anomalies in dense matter, *Phys. Rev. D* **70**, 074018 (2004) doi:10.1103/PhysRevD.70.074018 [arXiv:hep-ph/0405216 [hep-ph]].
- [21] S. P. Klevansky, The Nambu-Jona-Lasinio model of quantum chromodynamics, *Rev. Mod. Phys.* **64**, 649-708 (1992) doi:10.1103/RevModPhys.64.649
- [22] S. P. Klevansky and R. H. Lemmer, Chiral symmetry restoration in the Nambu-Jona-Lasinio model with a constant electromagnetic field, *Phys. Rev. D* **39**, 3478-3489 (1989) doi:10.1103/PhysRevD.39.3478
- [23] H. Suganuma and T. Tatsumi, Chiral symmetry and quark - anti-quark pair creation in a strong color electromagnetic field, *Prog. Theor. Phys.* **90**, 379-404 (1993) doi:10.1143/PTP.90.379
- [24] B. C. Tiburzi, Hadrons in Strong Electric and Magnetic Fields, *Nucl. Phys. A* **814**, 74-108 (2008) doi:10.1016/j.nuclphysa.2008.10.010 [arXiv:0808.3965 [hep-ph]].
- [25] W. R. Tavares and S. S. Avancini, Schwinger mechanism in the SU(3) Nambu-Jona-Lasinio model with an electric field, *Phys. Rev. D* **97**, no.9, 094001 (2018) doi:10.1103/PhysRevD.97.094001 [arXiv:1801.10566 [hep-ph]].
- [26] W. R. Tavares, R. L. S. Farias and S. S. Avancini, Deconfinement and chiral phase transitions in quark matter with a strong electric field, *Phys. Rev. D* **101**, no.1, 016017 (2020) doi:10.1103/PhysRevD.101.016017 [arXiv:1912.00305 [hep-ph]].
- [27] M. Ruggieri, Z. Y. Lu and G. X. Peng, Influence of chiral chemical potential, parallel electric, and magnetic fields on the critical temperature of QCD, *Phys. Rev. D* **94**, no.11, 116003 (2016) doi:10.1103/PhysRevD.94.116003 [arXiv:1608.08310 [hep-ph]].
- [28] M. Ruggieri and G. X. Peng, Quark matter in a parallel electric and magnetic field background: Chiral phase transition and equilibration of chiral density, *Phys. Rev. D* **93**, no.9, 094021 (2016) doi:10.1103/PhysRevD.93.094021 [arXiv:1602.08994 [hep-ph]].
- [29] E. B. S. Corrêa, Phase transition in a four-fermion interaction model under boundary conditions and electromagnetic effects, *Phys. Rev. D* **108**, no.7, 076002 (2023) doi:10.1103/PhysRevD.108.076002
- [30] W. R. Tavares, S. S. Avancini and R. L. S. Farias, Quark matter under strong electric fields in the linear sigma model coupled with quarks, *Phys. Rev. D* **108**, no.1, 016017 (2023) doi:10.1103/PhysRevD.108.016017 [arXiv:2305.07188 [hep-ph]].
- [31] A. Ahmad, Chiral symmetry restoration and deconfinement in the contact interaction model of quarks with parallel electric and magnetic fields, *Chin. Phys. C* **45**, no.7, 073109 (2021) doi:10.1088/1674-1137/abfb5f [arXiv:2009.09482 [hep-ph]].
- [32] J. C. Yang, X. Zhang and J. X. Chen, Study of the effects of external imaginary electric field and chiral chemical potential on quark matter, *Eur. Phys. J. C* **84**, no.7, 746 (2024) doi:10.1140/epjc/s10052-024-13069-x [arXiv:2309.09281 [hep-lat]].
- [33] A. Yamamoto, Lattice QCD with strong external electric fields, *Phys. Rev. Lett.* **110**, no.11, 112001 (2013) doi:10.1103/PhysRevLett.110.112001 [arXiv:1210.8250 [hep-lat]].
- [34] G. Endrodi and G. Marko, QCD phase diagram and equation of state in background electric fields, *Phys. Rev. D* **109**, no.3, 034506 (2024) doi:10.1103/PhysRevD.109.034506 [arXiv:2309.07058 [hep-lat]].
- [35] E. B. S. Corrêa and M. S. R. Sarges, Boundary conditions and electromagnetic effects on the phase transition of a zero spin bosonic system, [arXiv:2405.06095 [hep-th]].
- [36] M. Loewe, D. Valenzuela and R. Zamora, Catalysis and inverse electric catalysis in a scalar theory, *Phys. Rev. D* **105**, no.3, 036017 (2022) doi:10.1103/PhysRevD.105.036017 [arXiv:2112.13872 [hep-ph]].
- [37] M. Loewe and R. Zamora, Renormalons in a scalar self-interacting theory: Thermal, thermomagnetic, and thermoelectric corrections for all values of the temperature, *Phys. Rev. D* **105**, no.7, 076011 (2022) doi:10.1103/PhysRevD.105.076011 [arXiv:2202.08873 [hep-ph]].
- [38] M. Loewe, D. Valenzuela and R. Zamora, Effective potential and mass behavior of a self-interacting scalar field theory due to thermal and external electric and magnetic fields effects, *Eur. Phys. J. A* **59**, no.8, 184 (2023) doi:10.1140/epja/s10050-023-01097-2 [arXiv:2207.12387 [hep-ph]].
- [39] A. Okopinska, NONSTANDARD EXPANSION TECHNIQUES FOR THE EFFECTIVE POTENTIAL IN LAMBDA PHI**4 QUANTUM FIELD THEORY, *Phys. Rev. D* **35**, 1835-1847 (1987) doi:10.1103/PhysRevD.35.1835
- [40] A. Duncan and M. Moshe, Nonperturbative Physics from Interpolating Actions, *Phys. Lett. B* **215**, 352-358 (1988) doi:10.1016/0370-2693(88)91447-5
- [41] V. I. Yukalov, Interplay between Approximation Theory and Renormalization Group, *Phys. Part. Nucl.*

- 50, no.2, 141-209 (2019) doi:10.1134/S1063779619020047 [arXiv:2105.12176 [hep-th]].
- [42] F. F. de Souza Cruz, M. B. Pinto and R. O. Ramos, On the transition temperature for weakly interacting homogeneous Bose gases, *Phys. Rev. B* **64**, 014515 (2001) doi:10.1103/PhysRevB.64.014515 [arXiv:cond-mat/0007151 [cond-mat]].
- [43] H. Caldas, J. L. Kneur, M. B. Pinto and R. O. Ramos, Critical dopant concentration in polyacetylene and phase diagram from a continuous four-Fermi model, *Phys. Rev. B* **77**, 205109 (2008) doi:10.1103/PhysRevB.77.205109 [arXiv:0804.2675 [cond-mat.soft]].
- [44] H. Caldas and R. O. Ramos, Magnetization of planar four-fermion systems, *Phys. Rev. B* **80**, 115428 (2009) doi:10.1103/PhysRevB.80.115428 [arXiv:0907.0723 [cond-mat.soft]].
- [45] Y. M. P. Gomes, E. Martins, M. B. Pinto and R. O. Ramos, First-order phase transitions within Weyl type of materials at low temperatures, *Phys. Rev. B* **108**, no.8, 085107 (2023) doi:10.1103/PhysRevB.108.085107 [arXiv:2305.09007 [cond-mat.str-ell]].
- [46] J. L. Kneur, M. B. Pinto and R. O. Ramos, Thermodynamics and Phase Structure of the Two-Flavor Nambu–Jona-Lasinio Model Beyond Large- N_c , *Phys. Rev. C* **81**, 065205 (2010) doi:10.1103/PhysRevC.81.065205 [arXiv:1004.3815 [hep-ph]].
- [47] J. L. Kneur, M. B. Pinto, R. O. Ramos and E. Staudt, Vector-like contributions from Optimized Perturbation in the Abelian Nambu–Jona-Lasinio model for cold and dense quark matter, *Int. J. Mod. Phys. E* **21**, 1250017 (2012) doi:10.1142/S0218301312500176 [arXiv:1201.2860 [nucl-th]].
- [48] T. E. Restrepo, J. C. Macias, M. B. Pinto and G. N. Ferrari, Dynamical Generation of a Repulsive Vector Contribution to the Quark Pressure, *Phys. Rev. D* **91**, 065017 (2015) doi:10.1103/PhysRevD.91.065017 [arXiv:1412.3074 [hep-ph]].
- [49] D. C. Duarte, P. G. Allen, R. L. S. Farias, P. H. A. Manso, R. O. Ramos and N. N. Scoccola, BEC-BCS crossover in a cold and magnetized two color NJL model, *Phys. Rev. D* **93**, no.2, 025017 (2016) doi:10.1103/PhysRevD.93.025017 [arXiv:1510.02756 [hep-ph]].
- [50] K. G. Klimenko, Nonlinear optimized expansion and the Gross-Neveu model, *Z. Phys. C* **60**, 677-682 (1993) doi:10.1007/BF01558396
- [51] M. B. Pinto and R. O. Ramos, High temperature resummation in the linear delta expansion, *Phys. Rev. D* **60**, 105005 (1999) doi:10.1103/PhysRevD.60.105005 [arXiv:hep-ph/9903353 [hep-ph]].
- [52] M. B. Pinto and R. O. Ramos, A Nonperturbative study of inverse symmetry breaking at high temperatures, *Phys. Rev. D* **61**, 125016 (2000) doi:10.1103/PhysRevD.61.125016 [arXiv:hep-ph/9912273 [hep-ph]].
- [53] J. L. Kneur, M. B. Pinto, R. O. Ramos and E. Staudt, Updating the phase diagram of the Gross-Neveu model in 2+1 dimensions, *Phys. Lett. B* **657**, 136-142 (2007) doi:10.1016/j.physletb.2007.10.013 [arXiv:0705.0673 [hep-ph]].
- [54] J. L. Kneur, M. B. Pinto, R. O. Ramos and E. Staudt, Emergence of tricritical point and liquid-gas phase in the massless 2+1 dimensional Gross-Neveu model, *Phys. Rev. D* **76**, 045020 (2007) doi:10.1103/PhysRevD.76.045020 [arXiv:0705.0676 [hep-th]].
- [55] R. L. S. Farias, G. Krein and R. O. Ramos, Applicability of the Linear delta Expansion for the $\lambda\phi^4$ Field Theory at Finite Temperature in the Symmetric and Broken Phases, *Phys. Rev. D* **78**, 065046 (2008) doi:10.1103/PhysRevD.78.065046 [arXiv:0809.1449 [hep-ph]].
- [56] R. L. S. Farias, R. O. Ramos and D. S. Rosa, Symmetry breaking patterns for two coupled complex scalar fields at finite temperature and in an external magnetic field, *Phys. Rev. D* **104**, no.9, 096011 (2021) doi:10.1103/PhysRevD.104.096011 [arXiv:2109.03671 [hep-ph]].
- [57] M. C. Silva, R. O. Ramos and R. L. S. Farias, Phase transition patterns for coupled complex scalar fields at finite temperature and density, *Phys. Rev. D* **107**, no.3, 036019 (2023) doi:10.1103/PhysRevD.107.036019 [arXiv:2301.12621 [hep-ph]].
- [58] E. Martins, Y. M. P. Gomes, M. B. Pinto and R. O. Ramos, Testing the equivalence between the planar Gross-Neveu and Thirring models at $N = 1$, [arXiv:2407.03480 [hep-ph]].
- [59] J. L. Kneur, M. B. Pinto and R. O. Ramos, Convergent resummed linear delta expansion in the critical $O(N)$ ($\phi^2(i)$)* $2(3-d)$ model, *Phys. Rev. Lett.* **89**, 210403 (2002) doi:10.1103/PhysRevLett.89.210403 [arXiv:cond-mat/0207089 [cond-mat]].
- [60] D. S. Rosa, R. L. S. Farias and R. O. Ramos, Reliability of the optimized perturbation theory in the 0-dimensional $O(N)$ scalar field model, *Physica A* **464**, 11-26 (2016) doi:10.1016/j.physa.2016.07.067 [arXiv:1604.00537 [hep-ph]].
- [61] D. C. Duarte, R. L. S. Farias and R. O. Ramos, Optimized perturbation theory for charged scalar fields at finite temperature and in an external magnetic field, *Phys. Rev. D* **84**, 083525 (2011) doi:10.1103/PhysRevD.84.083525 [arXiv:1108.4428 [hep-ph]].
- [62] J. S. Schwinger, On gauge invariance and vacuum polarization, *Phys. Rev.* **82**, 664-679 (1951) doi:10.1103/PhysRev.82.664
- [63] J. Schwinger, The Theory of Quantized Fields. 5, *Phys. Rev.* **93**, 615-628 (1954) doi:10.1103/PhysRev.93.615
- [64] J. Schwinger, The Theory of Quantized Fields. VI, *Phys. Rev.* **94**, 1362-1384 (1954) doi:10.1103/PhysRev.94.1362
- [65] P. M. Stevenson, Optimized Perturbation Theory, *Phys. Rev. D* **23**, 2916 (1981) doi:10.1103/PhysRevD.23.2916
- [66] A. Ahmad, N. Ahmadiaz, O. Corradini, S. P. Kim and C. Schubert, Master formulas for the dressed scalar propagator in a constant field, *Nucl. Phys. B* **919**, 9-24 (2017) doi:10.1016/j.nuclphysb.2017.03.007 [arXiv:1612.02944 [hep-ph]].
- [67] J. P. Edwards and C. Schubert, One-particle reducible contribution to the one-loop scalar propagator in a constant field, *Nucl. Phys. B* **923**, 339-349 (2017) doi:10.1016/j.nuclphysb.2017.08.002 [arXiv:1704.00482 [hep-th]].
- [68] G. V. Dunne, Heisenberg-Euler effective Lagrangians: Basics and extensions, doi:10.1142/9789812775344_0014 [arXiv:hep-th/0406216 [hep-th]].
- [69] T. D. Cohen and D. A. McGady, The Schwinger mechanism revisited, *Phys. Rev. D* **78**, 036008 (2008) doi:10.1103/PhysRevD.78.036008 [arXiv:0807.1117 [hep-

- ph]].
- [70] E. J. Weinberg and A. q. Wu, UNDERSTANDING COMPLEX PERTURBATIVE EFFECTIVE POTENTIALS, *Phys. Rev. D* **36**, 2474 (1987) doi:10.1103/PhysRevD.36.2474
- [71] G. Piccinelli, A. Sanchez, A. Ayala and A. J. Mizher, Warm inflation in presence of magnetic fields, *AIP Conf. Proc.* **1548**, no.1, 288-293 (2013) doi:10.1063/1.4817059 [arXiv:1311.0533 [astro-ph.CO]].
- [72] A. P. Prudnikov, Yu A. Brychkov and O. I Marichev, Integrals and series, Volume 1: Elementary functions. (Gordon&Breach Sci. Publ., New York, 1986).
- [73] B. B. Brandt, G. Endrődi, J. J. H. Hernández, G. Markó and L. Pannullo, Electromagnetic effects on topological observables in QCD, *PoS LATTICE2023*, 188 (2024) doi:10.22323/1.453.0188 [arXiv:2312.14660 [hep-lat]].
- [74] G. S. Bali, B. B. Brandt, G. Endrődi and B. Gläbke, Meson masses in electromagnetic fields with Wilson fermions, *Phys. Rev. D* **97**, no.3, 034505 (2018) doi:10.1103/PhysRevD.97.034505 [arXiv:1707.05600 [hep-lat]].
- [75] H. T. Ding, S. T. Li, J. H. Liu and X. D. Wang, Chiral condensates and screening masses of neutral pseudoscalar mesons in thermomagnetic QCD medium, *Phys. Rev. D* **105**, no.3, 034514 (2022) doi:10.1103/PhysRevD.105.034514 [arXiv:2201.02349 [hep-lat]].
- [76] M. Loewe and J. C. Rojas, Thermal effects and the effective action of quantum electrodynamics, *Phys. Rev. D* **46**, 2689-2694 (1992) doi:10.1103/PhysRevD.46.2689
- [77] P. Elmfors and B. S. Skagerstam, Electromagnetic fields in a thermal background, *Phys. Lett. B* **348**, 141-148 (1995) [erratum: *Phys. Lett. B* **376**, 330-330 (1996)] doi:10.1016/0370-2693(95)00124-4 [arXiv:hep-th/9404106 [hep-th]].
- [78] J. Hallin and P. Liljenberg, Fermionic and bosonic pair creation in an external electric field at finite temperature using the functional Schrodinger representation, *Phys. Rev. D* **52**, 1150-1164 (1995) doi:10.1103/PhysRevD.52.1150 [arXiv:hep-th/9412188 [hep-th]].
- [79] A. K. Ganguly, J. C. Parikh and P. K. Kaw, Thermal tunneling of q anti-q pairs in A-A collisions, *Phys. Rev. C* **51**, 2091-2094 (1995) doi:10.1103/PhysRevC.51.2091
- [80] A. K. Ganguly, Comment on fermionic and bosonic pair creation in an external electric field at finite temperature, [arXiv:hep-th/9804134 [hep-th]].
- [81] H. Gies, QED effective action at finite temperature, *Phys. Rev. D* **60**, 105002 (1999) doi:10.1103/PhysRevD.60.105002 [arXiv:hep-ph/9812436 [hep-ph]].
- [82] H. Gies, QED effective action at finite temperature: Two loop dominance, *Phys. Rev. D* **61**, 085021 (2000) doi:10.1103/PhysRevD.61.085021 [arXiv:hep-ph/9909500 [hep-ph]].
- [83] L. Medina and M. C. Ogilvie, Schwinger Pair Production at Finite Temperature, *Phys. Rev. D* **95**, no.5, 056006 (2017) doi:10.1103/PhysRevD.95.056006 [arXiv:1511.09459 [hep-th]].
- [84] O. Gould and A. Rajantie, Thermal Schwinger pair production at arbitrary coupling, *Phys. Rev. D* **96**, no.7, 076002 (2017) doi:10.1103/PhysRevD.96.076002 [arXiv:1704.04801 [hep-th]].
- [85] M. Korwar and A. M. Thalappilil, Finite temperature Schwinger pair production in coexistent electric and magnetic fields, *Phys. Rev. D* **98**, no.7, 076016 (2018) doi:10.1103/PhysRevD.98.076016 [arXiv:1808.01295 [hep-th]].